THE JOURNAL OF BIOLOGICAL CHEMISTRY
Vol. 275, No. 12, Issue of March 24, pp. 8779–8784, 2000

Printed in U.S.A.

Phragmoplastin Polymerizes into Spiral Coiled Structures via Intermolecular Interaction of Two Self-assembly Domains*

(Received for publication, October 5, 1999, and in revised form, November 4, 1999)

Zhongming Zhang, Zonglie Hong, and Desh Pal S. Verma‡

From the Department of Molecular Genetics and Plant Biotechnology Center, The Ohio State University, Columbus, Ohio 43210-1002

Phragmoplastin, a high molecular weight GTPase belonging to the dynamin superfamily of proteins, becomes associated with the cell plate during cytokinesis in plants. Growth of the cell plate requires continuous fusion of vesicles, and phragmoplastin appears to play a role in the formation of vesicle-tubule-vesicle structures at the cell plate. In this study, we have demonstrated that two self-assembly domains (SA1 and SA2) are involved in polymerization of phragmoplastin. SA1 is about 42 amino acids long and is located near the N terminus overlapping with the GTP-binding region. SA2, containing at least 24 amino acids, is located in the middle of the molecule outside the GTP-binding domain. Peptides containing either SA1 or SA2 interact efficiently with the full-length phragmoplastin. The SA1 domain of one phragmoplastin molecule also binds to SA2 of another as confirmed *in vitro* by using radiolabeled peptides. This interaction leads to the formation of polymers with a staggered contoured spiral structure. Electron microscopy studies revealed that helical arrays of phragmoplastin can be induced by reducing salt concentration. Our results suggest that phragmoplastin may assemble into helical arrays that wrap around and squeeze vesicles into vesicle-tubule-vesicle structures observed on the forming cell plate.

Phragmoplastin is a GTPase with molecular mass of 68 kDa and shares significant overall amino acid sequence similarity, particularly in the N-terminal half, with the members of the dynamin superfamily. Dynamin-like proteins have been isolated from a variety of eukaryotes, ranging from yeast to plants to humans. These proteins are mostly membrane-bound with different subcellular locations and have been implicated in diverse biological processes, including vesicle formation, protein sorting, resistance to viral infection, mitochondrial and chloroplast biogenesis, endocytosis, and cell plate formation (1–5). Phragmoplastin was shown to be specifically associated with cell plate during cytokinesis in plants (1, 6). Three *Arabidopsis* cDNAs encoding dynamin-like proteins (aG68, ADL1, and ADL2) have been identified, of which ADL1 and ADL2 have been implicated in chloroplast biogenesis (3, 7, 8). Similar to yeast Vps1 and human Drp1 (4, 9, 10), phragmoplastin lacks a C-terminal proline-rich domain that interacts with Src homology 3 (SH3) proteins (11). Phragmoplastin also lacks the pleckstrin homology (PH) domain that mediates the binding of dynamin to membranes containing acidic phospholipids (12).

Ability to self-assemble into helical arrays is one of the common features shared by dynamin family of proteins. One class of the dynamin homologues, Mx proteins, can polymerize into helical structures that are 11 nm thick and 100–150 nm long (13). Mx proteins contain a "self-assembly" domain that is conserved in the dynamin family of proteins (14), including phragmoplastin (1). Dynamins can form helical structures both in solution and *in vivo* (15, 16). This property enables dynamin to wrap around the base of clathrin-coated pits and constricts their neck upon addition of GTP (17, 18). Dynamin alone is sufficient for the formation of constricted necks of coated pits (17). By hydrolyzing GTP, it functions as a force-generating molecule responsible for the fission of membrane vesicles. The presence of lipid promotes the formation of polymeric complexes of dynamin (15). Self-assembly of dynamin does not require guanine nucleotides, but GTP binding promotes self-assembly, whereas GTP hydrolysis may trigger disassembly of dynamin polymers (17). Assembly of dynamin into spirals can be induced by the addition of GDP and γ-phosphate analogues under physiological conditions (19). Multiple peptide domains have been implicated in self-assembly of dynamin and its homolog proteins, including Dnm1p/Vps1p-like (DVLP). Whereas the C-terminal proline rich domain of dynamin is not required for self-assembly (19), DVLP contains a conserved domain DVH2 (for Dnm1/Vps1 homology 2) at the C terminus that is involved in oligomerization of DVLP (20). The process of dynamin self-assembly may be accounted for by both intra- and intermolecular interactions between three different protein domains (21). Coiled-coils have also been demonstrated to be involved in dynamin self-assembly (22). However, they may not play a role in phragmoplastin self-assembly, because the probability of coiled-coil formation in phragmoplastin is very low (only 20%). These data suggest that members of the dynamin family may form helical structures using different domains that provide intra- and intermolecular interactions.

Assembly and disassembly of dynamin-like proteins on the surface of biological membranes may provide a mechanism to control vesicle budding, vesicle fusion, and the formation of new membrane systems, such as vesicle-tubule-vesicle structures, that occur during cell plate formation. Phragmoplastin appears to be a "simpler" molecule than dynamin and Mx proteins because it does not contain the proline-rich domain or leucine zipper at the C terminus and lacks the pleckstrin homology domain. Nevertheless, this protein retains the ability to form oligomers of its own and forms complexes with other proteins (6).[1] Using a yeast two-hybrid system in combination with an *in vitro* protein-protein interaction assay, we identified two domains that are involved in phragmoplastin oligomeriza-

* This work was supported by National Science Foundation Grant IBN-9724014. The costs of publication of this article were defrayed in part by the payment of page charges. This article must therefore be hereby marked "*advertisement*" in accordance with 18 U.S.C. Section 1734 solely to indicate this fact.

‡ To whom correspondence should be addressed: Plant Biotechnology Center, 1060 Carmack Rd., Columbus, OH 43210-1002 Tel.: 614-292-3625; Fax: 614-292-5379; E-mail: verma.1@osu.edu.

[1] Z. Hong, Z. Zhang, and D. P. S. Verma, unpublished data.

tion leading to the formation of helical arrays that may facilitate formation of vesicle-tubule-vesicle structures at the cell plate.

EXPERIMENTAL PROCEDURES

Bacteria and Yeast Strains—Escherichia coli DH5α and Top10F′ were used for plasmid construction. HB101 was used to recover plasmids from yeast cells. Yeast (*Saccharomyces cerevisiae*) Y190 (*MATa*, *ura3–52, his3–200, lys2–801, ade2–101, trp1–901, leu2–3, 112, gal4*Δ, *gal80*Δ, *cyh*^{r}*2*, *LYS*::*GAL1*$_{UAS}$-*HIS3*$_{TATA}$-*HIS3*, *URA3*::*GAL1*$_{UAS}$-*GAL1*$_{TATA}$-*lacZ*) was used as the host for two-hybrid experiments.

Plasmid Construction—Full-length phragmoplastin cDNA (pSDL12a) (1) was partially digested with *Bgl*II and *Xho*I, and the 2-kb[2] fragment was ligated into the pAS1-CYH2 and pACT2 vectors, generating pAS-Phr and pACT-Phr, respectively. The *Bgl*II-*Xho*I fragment was also inserted at the *Bam*HI-*Sal*I sites of pUC18. The resulting plasmid (pUC-Phr) was digested with *Sma*I-*Bam*HI, and the insert was subcloned into the same sites of pACT2, generating pACT-BH1. pACT-BL2 expressing the SA1 domain of phragmoplastin was constructed by subcloning a *Sma*I-*Bgl*II fragment (0.57 kb) from pUC-Phr into the *Sma*I-*Bam*HI sites of pACT2. A *Hinc*II fragment was released from pUC-Phr, followed by self-ligation, generating pUC-HC2Δ. pACT-HC2 containing the SA2 domain was made by subcloning a *Sma*I-*Bam*HI fragment (0.9 kb) into pACT2. For construction of pACT-H3, a *Sma*I-*Hin*dIII fragment (0.75 kb) was transferred from pUC-HC2Δ to pBluescript II SK(−) to give pBS-HC2Δ, from which a *Sma*I-*Xho*I fragment was subcloned into the same sites of pACT2. pACT-DR1 was constructed by cloning a *Dra*I-*Bam*HI fragment (0.62 kb) into the *Sma*I-*Bam*HI sites of pACT2.

Yeast Two-hybrid Assay—To assay protein-protein interaction, cDNAs encoding the respective peptides were subcloned into pAS2 in-frame with the DNA-binding domain of Gal4 and into pACT2 in-frame with the transcription activation domain. Yeast Y190 was transformed with the two plasmids by electroporation followed by selection on yeast synthetic complete medium (SC-Trp-Leu). Colonies were transferred to interaction medium (SC-Trp-Leu-His containing 30 mg/liter 3-amino-1,2,4-triazole). Colonies growing on SC-Trp-Leu medium were adsorbed to 3MM filter discs, permeabilized by liquid nitrogen, and incubated in Z buffer/X-Gal (120 mM sodium phosphate, pH 7.0, 10 mM KCl, 1 mM $MgCl_2$, 0.2 mM β-mercarptoethanol, 300 mg/liter X-Gal). Development of blue/white color was scored 2–10 h later.

β-Galactosidase Assay—Yeast cells grown in liquid selection medium containing 2% raffinose were pelleted and washed twice with phosphate-saline buffer. The pellet was resuspended in a lysis solution (100 mM potassium phosphate, pH 7.8, 0.2% Triton X-100, 1 mM dithiothreitol). After incubation at 4 °C for 20 min, cells were permeabilized by two freeze-thaw cycles (23). Cell extracts were added to a reaction buffer (3 mM methyl-umbelliferyl-β-D-galactopyranoside in 100 mM sodium phosphate, pH 7.0, 1 mM $MgCl_2$). After incubation for 60 min at 37 °C, the reaction was terminated by the addition of an equal volume of stop buffer (300 mM glycine, 15 mM EDTA, pH 11.5). The mixture was diluted, and fluorescence was recorded in a fluorometer (24).

Screening of cDNA Library Using Two-Hybrid System—pAS-Phr expressing the full-length phragmoplastin was used as a bait to screen an *Arabidopsis* cDNA library constructed in the λ-ACT vector (25). One of the interacting clones, pACT-AtC, contained a partial fragment of the ADL1 cDNA and was sequenced.

Purification of GST Fusion Proteins—A full-length phragmoplastin was fused with GST by inserting the *Sma*I-*Xho*I fragment from pACT-Phr into the same sites of pGEX-KG (26), generating pGST-Phr. A *Sma*I-*Eco*RI fragment from pACT-BL2 encoding the SA1 domain was ligated into the same sites of pGEX-KG, generating pGST-SA1. Plasmid pGST-SA2 was constructed by subcloning a *Sma*I-*Eco*RI fragment from pACT-HC2 into the same sites of pGEX-KG. Expression of GST fusion proteins was induced by 1 mM isopropyl-1-thio-β-D-galactopyranoside for 4 h. Cells were washed and resuspended in STE buffer (10 mM Tris-Cl, pH 8.0, 150 mM NaCl, 1 mM EDTA). After incubation with 100 μg/ml lysozyme for 5 min, cells were lysed in the presence of 0.5% sarkosyl followed by sonication (27). The supernatant was diluted with Triton X-100 to a final concentration of 1% and incubated with glutathione-agarose-beads (Sigma) followed by extensive washing with STE buffer.

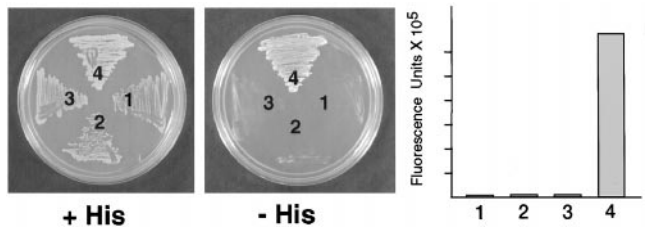

FIG. 1. **Self-interaction of phragmoplastin in the yeast two-hybrid system.** Yeast cells harboring different combinations of plasmids were streaked on synthetic media with or without histidine. Yeast cell extracts were assayed for β-galactosidase activity, and average values from four independent assays are presented (*right panel*). *Column 1,* cells containing two empty vectors; *column 2,* pAS-Phr; *column 3,* pACT-Phr; *column 4,* phragmoplastin fused with DNA-binding and transcription activation domains (pAS-Phr and pACT-Phr, respectively), allowing self-assembly of phragmoplastin.

In Vitro Protein-Protein Interaction Assay—A ^{35}S-labeled peptide containing the SA2 domain was obtained by subcloning a *Bam*HI fragment from pGST-SA2 into the same site of pAGA3 (Promega, Madison, WI) in-frame with the vector ATG initiation codon under the T7 promoter. The resulting construct, pAGA3-SA2, was used for TNT-T7 Quick-Coupled Transcription/Translation System (Promega) in the presence of [^{35}S]methionine. Radiolabeled SA2 product (10 μl) was diluted in 260 μl of interaction buffer (20 mM Tris-Cl, pH 8.0, 100 mM KCl, 2 mM $MgCl_2$, 0.5% lubral, 0.5% bovine serum albumin) and incubated with 10 μl of purified GST fusion protein bound to glutathione-agarose-beads for 1 h. The beads were washed five times with the interaction buffer without bovine serum albumin, and the bound proteins were eluted directly in SDS-polyacrylamide gel electrophoresis sample buffer. After electrophoresis, the gel was stained with Coomassie Blue R-250, dried, and autoradiographed.

Negative-stain Electron Microscopy—GST-phragmoplastin, purified by glutathione-agarose beads (Sigma), was eluted with 10 mM reduced glutathione in HCB (20 mM Hepes, pH 7.2, 2 mM EGTA, 1 mM $MgCl_2$, 1 mM dithiothreitol) containing 150 mM NaCl (HCB150, high salt buffer). Glutathione was removed by passing through a Sephadex G25 column in high salt buffer. The sample was dialyzed against a low salt buffer (HCB15, HCB containing 15 mM NaCl) overnight at 4 °C. Dialyzed phragmoplastin was incubated with 10 μM GTPγS or GTP for 30 min. Samples (~ 0.1 mg/ml protein) were adsorbed to Formvar-coated grids and stained with 2% uranyl acetate followed by air drying. Electron micrographs were obtained using a Philips 400 electron microscope at 80 kV.

RESULTS

Intermolecular Interaction of Phragmoplastin in the Yeast Two-hybrid System—Using a cross-linking approach, we previously reported that soybean phragmoplastin forms homo-oligomers (6). This was explained by the presence in phragmoplastin of a self-assembly domain similar to that described in Mx proteins (28). During the course of screening for phragmoplastin-interacting proteins using the yeast two-hybrid system, we isolated from an *Arabidopsis* library several isoforms of phragmoplastin-like proteins that lacked the N-terminal half of the molecule, where the self-assembly domain is located. These results suggested that an additional domain(s) must exist in the second half of the protein that allows intermolecular interaction. We subcloned soybean phragmoplastin cDNA in both pAS2 and pACT2 and determined the domains involved in the assembly of phragmoplastin that can be assayed using the two-hybrid system. Data in Fig. 1 demonstrate that cells expressing phragmoplastin from both vectors grow well on His$^-$ SC medium containing 30 mM of SC-Trp-Leu-His and 30 mg/liter 3-amino-1,2,4-triazole, suggesting that an interaction occurs between phragmoplastin molecules. When phragmoplastin was fused only with the DNA-binding domain in pAS2, or only with the transcription activation domain in pACT2, or when two empty vectors were used, the yeast cells were not

[2] The abbreviations used are: SA1, self-assembly domain 1; SA2, self-assembly domain 2; pAS-Phr, full-length phragmoplastin fused with the DNA-binding domain; pACT-Phr, phragmoplastin fused with transcription activation domain; ACT, activation domain; Gal, galactosidase; GST, glutathione *S*-transferase; GTPγS, guanosine 5′-3-*O*-(thio-)triphosphate; kb, kilobase(s); SC, synthetic complete medium.

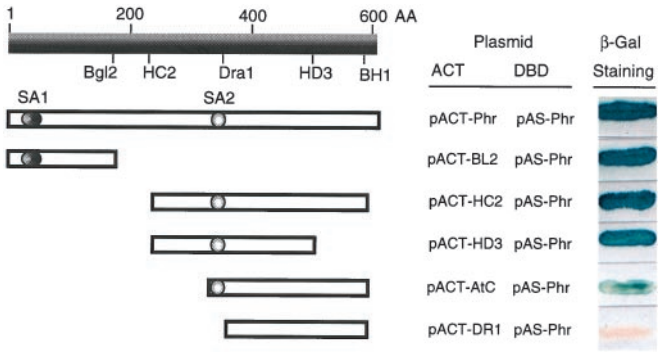

FIG. 2. **Delimitation of peptide domains required for phragmoplastin self-assembly.** Soybean phragmoplastin cDNA (pSDL12A) (1) digested with restriction enzymes was fused in-frame with the DNA-binding domain (*DBD*) in the pAS2 vector and transferred into yeast cells that express a full-length phragmoplastin fused with the transcription activation domain (*ACT*) of pACT2. Transformants from each strain were streaked on X-Gal plates.

able to grow on His^- SC medium. The self-interaction was very strong, as revealed by X-Gal reaction that took less than 1 h to develop blue color (data not shown). β-Galactosidase activity assays produced consistent results with His selection experiments and X-Gal reaction. This interaction was equally strong when the self-assembly domain was missing (see below), suggesting the presence of a new domain that has not yet been described in the dynamin family of proteins.

Two Self-assembly Domains Are Involved in the Polymerization of Phragmoplastin—A set of deletion constructs were made to delimit peptide domains required for self-interaction of phragmoplastin. The *Bgl*II fragment (amino acids 1–185) contains a peptide domain (amino acids 49–93) that was previously thought to be responsible for phragmoplastin self-interaction because this domain is homologous to the self-assembly domain (amino acids 51–96) of mouse Mx1 protein (13). The deletion fragments were subcloned in pACT2 vector in-frame with the transcription activation domain of Gal4 (Fig. 2). For interaction, full-length phragmoplastin was fused with the DNA-binding domain (pAS-Phr). As expected, phragmoplastin was able to interact with the peptide encoded by the *Bgl*II fragment, suggesting that this region contains SA1 (Fig. 3*A*). The peptides encoded by the *Hinc*II and *Hin*dIII fragments, respectively, which lacked the SA1 domain, were also able to efficiently interact with the full-length phragmoplastin, whereas the *Dra*I fragment-generated peptide completely lost the interaction ability. pACT-AtC obtained from library screening using the full-length phragmoplastin as a bait (see under "Experimental Procedures") is a partial ADL1 clone that is 72 base pairs longer than the *Dra*I fragment at the 5′ end, encoding 24 amino acids. This suggests that the peptide between amino acid residues 347–371 of phragmoplastin represents a new self-assembly domain (referred as SA2). Amino acid sequence comparison of the SA2 domain with members of the dynamin family revealed a limited homology in this region (Fig. 3*B*). The role of SA2 homologous domains in the polymerization of dynamin and Mx proteins remains to be determined (see under "Discussion"). The data also suggested that the C-terminal 30 amino acids are not involved in self-assembly, because removal of this region did not affect the interaction (pACT-BH1).

Interaction between the Two Self-assembly Domains—To test whether SA1 interacts only with itself or whether it interacts with SA2 of another molecule, and to eliminate possible effects of vectors, we subcloned the *Bgl*II and *Hinc*II fragments, respectively, in both vectors (pAS2 and pACT2) and tested different combinations of the plasmids in the two-hybrid system. Full-length phragmoplastin served as a positive control in this experiment. Fig. 4 shows that SA1 does not have binding affinity toward itself but interacts with SA2. SA2, on the other hand, may interact with itself and SA1. To exclude the possibility that SA2 region may activate transcription on its own, we used "empty" vector pACT2 as a negative control plasmid along with pAS-SA2 to transform the yeast cells. These cells were negative in X-Gal assay, suggesting that SA2 cannot act as a transcription activator and that the X-Gal staining is brought about through protein-protein interaction. Although the importance of SA2-SA2 interaction in phragmoplastin polymerization is not clear at this point, the interaction between SA1 and SA2 could be significant as it may provide a novel mechanism for the formation of phragmoplastin polymers in a staggered helical array (see under "Discussion").

To test whether any other protein component(s) may be required for the interaction between two phragmoplastin fragments, we used radiolabeled peptide from *in vitro* translated SA2 to react with purified phragmoplastin deletion fragments. Full-length phragmoplastin and the *Bgl*II and *Hinc*II fragments were cloned in pGEX-KG vector in-frame with GST. The recombinant proteins were expressed in *E. coli* and purified as GST fusion proteins using glutathione-agarose beads. The ^{35}S-labeled peptides were obtained by *in vitro* translation and were reacted with purified GST fusion proteins bound to glutathione-agarose beads. As shown in Fig. 5, GST alone did not react with ^{35}S-labeled SA2. GST fusion with SA1, SA2, and the full-length phragmoplastin interacted with ^{35}S-labeled SA2 product, suggesting that SA2 can interact with SA1, SA2, and the full-length phragmoplastin. These results are consistent with that obtained *in vivo* using the yeast two-hybrid system and provide further evidence for the intermolecular interaction between SA1 and SA2 domains. More importantly, this experiment demonstrated that such an interaction occurs through direct contact and that no additional protein is required.

Phragmoplastin Assembles into Helical Structures—Purified phragmoplastin under high salt conditions (HCB150) did not polymerize and appeared to exist predominantly as monomers and dimers, as shown by negative-stain electron micrographs (Fig. 6*A*). Polymerization could be induced by dialysis against a low salt buffer (HCB15; Fig. 6, *B* and *D*). The presence of 10 μM GTP reversed the polymerization process and disassembled the helical structures into oligomers (data not shown). Incubation with GTPγS, a nonhydrolyzable analog of GTP, maintained the helical structures, suggesting that hydrolysis of GTP by phragmoplastin GTPase results in disassembly of helical arrays. Comparison of the helical arrays formed with or without the presence of GTPγS revealed that addition of GTPγS makes the helical arrays into more compact structures (Fig. 6, *B* and *C*). These results may be improved by using native phragmoplastin peptides. These data demonstrate that assembly of phragmoplastin into higher order helical structures can be induced by reducing salt concentration in the buffer without the presence of GTP. Hydrolysis of GTP appears to alter the stereo-structure of helical arrays and disassembles the arrays into oligomers.

DISCUSSION

Identification of Two Self-assembly Domains Involved in Polymerization of Phragmoplastin—Members of the dynamin family including phragmoplastin have been shown to form polymers. These polymers are formed in a highly ordered manner, a process known as self-assembly. The process of self-assembly can be demonstrated *in vitro*. Native dynamin can be extracted in high salt (300 mM NaCl) buffer. When salt concentrations were reduced to 25–50 mM by dialysis, dynamin spontaneously self-assembled into a mixture of partial rings, intact rings, and small stacks of interconnected rings (15). The ring

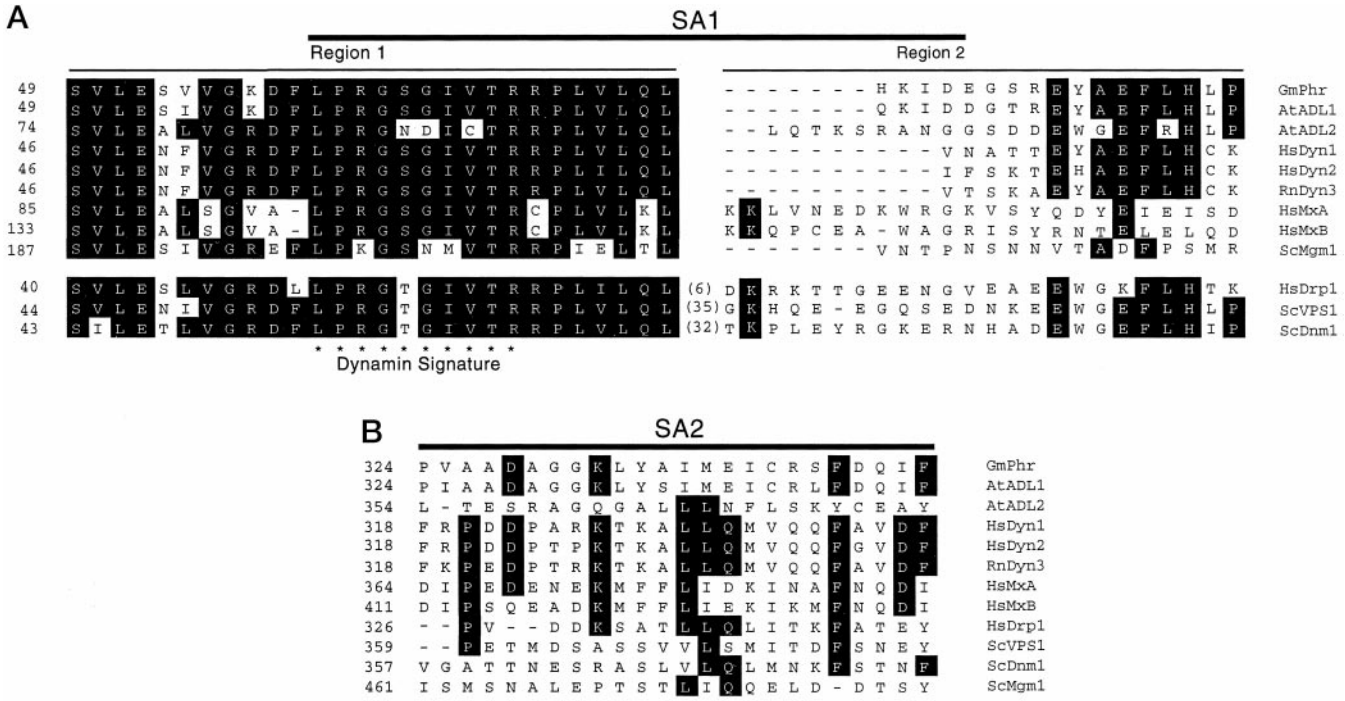

FIG. 3. **Alignment of amino acid sequences of the two self-assembly domains of phragmoplastin and their homologous regions in the dynamin protein family.** Amino acid sequences of soybean phragmoplastin (*GmPhr*), *Arabidopsis* dynamin-like protein 1 (AtADL1) (GenBank™ accession number L36939), AtADL2 (AF012833), human dynamin 1 (HsDyn1) (L07807), HsDyn2 (L36983), rat dynamin 3 (RnDyn3) (D14076), human MxA (HsMxA) (M30817), HsMxB (M30818), human dynamin-related protein 1 (HsDRP1) (AF000430), yeast Vps1 (ScVps1) (P21576), ScDnm1 (L40588), and ScMgm1 (X62834) were aligned using DNA Star software. The aligned regions corresponding to phragmoplastin amino acid residues 51–96 and 347–371 are presented in *A* (SA1 domain) and *B* (SA2 domain), respectively. In *parentheses* are numbers of amino acid residues that were omitted to maximize the alignment. The dynamin signature motif is marked by *asterisks*. Positions of the first amino acid residues of SA1 and SA2 in the proteins are indicated on the *left*.

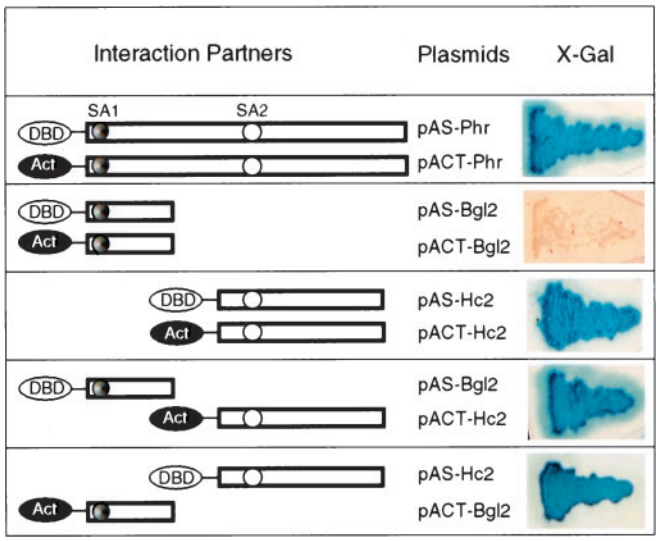

FIG. 4. ***In vivo* interaction between the two self-assembly domains (SA1 and SA2) of phragmoplastin.** *Bgl*II and *Hin*cII fragments containing SA1 and SA2, respectively, from the phragmoplastin cDNA were fused in-frame in pAS2 and pACT2. Plasmids containing full-length phragmoplastin in both vectors were used as positive controls. Yeast transformants were selected on Leu$^-$-Trp$^-$ media and streaked on X-Gal plates. Yeast cells containing pAS-SA2 and empty vector pACT2 (negative control) did not turn blue in X-Gal staining (data not shown).

stacks can further assemble into striking tubules of dynamin that can be reversibly disassembled into simple structures. Similar helical arrays of dynamin have also been observed *in vivo*, being bound to microtubules (29, 30), or as coats surrounding tubular membrane invaginations in nerve terminals (16, 31). We dissected the structural components required for self-assembly of phragmoplastin and demonstrated here that two self-assembly domains (SA1 and SA2) are involved in this process. One of them, SA1, is homologous to the so-called self-assembly domain identified in Mx1 and other dynamin family of proteins (14). SA1 is located between consensus sequence I (G*XXXX*GK(S/T)) and consensus II (D*XX*G) of the tripartite GTP-binding motif. SA1 is 48 amino acids long in mouse Mx1 but is 6 amino acids shorter in phragmoplastin. It consists of two parts: region 1 is highly conserved among members of the dynamin family and contains the "dynamin signature" motif (LP(R/G)(S/T/N)(G/N)IVTR). Region 2 of SA1 is variable in length and has little homology among dynamin-like proteins (Fig. 3). Our data demonstrated that SA2 (24 amino acids long) is necessary for phragmoplastin self-interaction. However, it is not clear whether this fragment of 24 amino acids alone is sufficient for the interaction. This region could be part of a longer domain. SA2 shows limited homology among dynamin-like proteins. It is not known whether the homologous SA2 domain in dynamins is indeed involved in self-assembly.

Phragmoplastin Forms Polymers through Staggered Interactions of Intermolecular SA1 and SA2 Domains—Human MxA contains a C-terminal leucine zipper that can interact with an internal region of the MxA molecule. Intermolecular interaction between the leucine zipper and the internal region leads to the formation of MxA polymers (32). Human dynamin, yeast Vps1, and plant phragmoplastin do not contain a leucine zipper but may use the SA2 domain instead. We do not have evidence so far for an intramolecular interaction between SA1 and SA2, which would otherwise cause a significant conformational change (N-terminal forward folding). Our results also suggest that the SA2 domains of two phragmoplastin molecules can interact with each other. The significance of such an interaction, if taking place *in planta*, also remains to be elucidated. In this report, we have presented evidence obtained both from

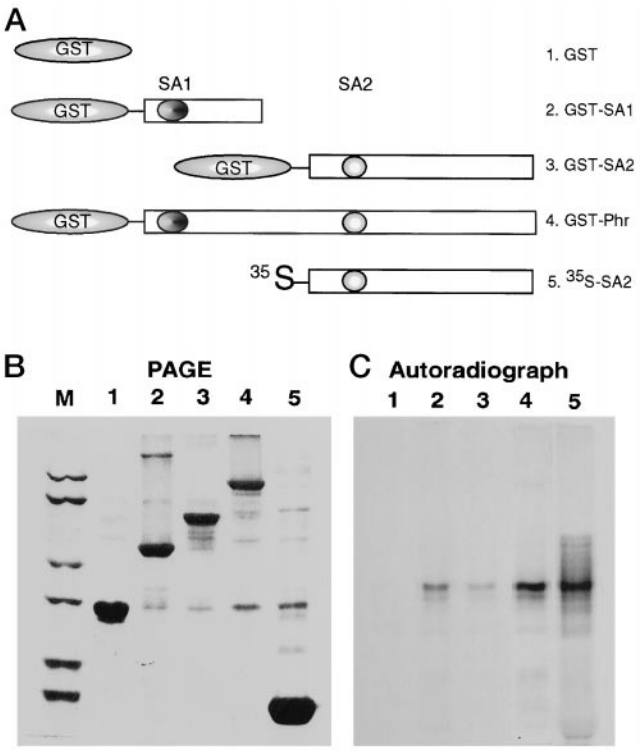

FIG. 5. ***In vitro* protein-protein interactions between two self-assembly domains of phragmoplastin.** Phragmoplastin cDNA fragments containing SA1 and SA2 domains, respectively, were expressed (see under "Experimental Procedures") as fusion proteins (*A, rows 2* and *3*). GST alone (*row 1*) and a fusion protein between GST and the full-length phragmoplastin (*row 4*) were used as negative and positive controls, respectively. The SA2 domain of phragmoplastin was also radiolabeled with [^{35}S]methionine using an *in vitro* transcription/translation system. An aliquot of the radiolabeled SA2 product was mixed with SDS-sample buffer and loaded in *row 5*. The rest of the radiolabeled product was used to react with purified SA1 or SA2 peptides that were adsorbed to glutathione-agarose beads. After extensive washing with the buffer, peptides retained on the beads were eluted with SDS sample buffer and resolved by SDS-polyacrylamide gel electrophoresis. The gel was stained with Coomassie Blue R-250 (*B*), dried, and autoradiographed (*C*). *M,* protein markers from Bio-Rad with molecular masses (from low to high) of 14, 21, 31, 45, 66, and 97 kDa. Lane numbers in *B* and *C* correspond to row numbers in *A*.

yeast two-hybrid system (*in vivo*) and *in vitro* experiments, to demonstrate that SA1 and SA2 interact intermolecularly with each other. Continuous interaction between SA1 of one molecule and SA2 of the other will lead to the formation of a staggered polymeric helical structure (Fig. 6*F*). The length of such structures may be controlled by GTP hydrolysis and interaction with other proteins.

Assembly and Disassembly of Phragmoplastin into Helical Arrays Is Regulated by GTP Hydrolysis—Whereas the exact molecular shape of the purified native phragmoplastin remains to be determined through x-ray crystallography, GST-fused phragmoplastin molecules do not appear to be "rod-shaped" as shown on negative stained electron micrographs (Fig. 6*A*). Interactions between SA1 and SA2 of neighboring molecules may lead to the formation of a helical array (Fig. 6*F*). Purified phragmoplastin indeed forms helical structures when the salt concentrations were reduced slowly by dialysis to 15 mM NaCl (Fig. 6). Such helical arrays can be disassembled by the presence of GTP (data not shown) but not GTPγS. Similar helical structures have also been observed in dynamin and Mx proteins *in vitro* and *in vivo* (15–17, 33). Assembly and disassembly of phragmoplastin in plant cells could be regulated by many other factors, such as lipid attachment, or through interaction with other proteins.

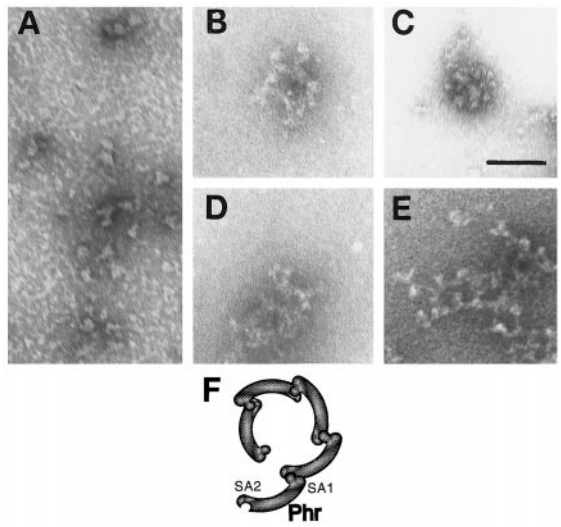

FIG. 6. **Negative-stained electron micrographs of phragmoplastin polymers.** Purified phragmoplastin proteins in high salt (HCB150) buffer (*A*) were dialyzed against a low salt (HCB15) buffer (*B* and *D*). Dialyzed phragmoplastin was incubated with 10 μM GTPγS (*C* and *E*). Face views (*B* and *C*) and side views (*D* and *E*) of assembled phragmoplastin rings are presented. Shown in *F* is a schematic model for the assembly of phragmoplastin into staggered helical polymers formed via SA1 and SA2 interactions. *Scale bar,* 100 nm.

Formation of Tubular Structures at the Cell Plate—Five morphological steps have been distinguished during cell plate formation: the transport of Golgi-derived vesicle to the equatorial region, the formation of thin dumbbell-shaped tubules, the consolidation of tubulovesicular network into a plate-like structure, the fusion of cell plate with the parental cell wall, and the deposition of cellulose on the cell plate (34). Phragmoplastin is detected immediately after the Golgi-derived vesicles begin to fuse to form the early cell plate. As the cell plate grows, phragmoplastin redistributes from the center to the growing edges of the outwardly expanding cell plate (6). The tight temporal and spatial correlation between the formation of the tubulovesicular network and the distribution of phragmoplastin suggests that phragmoplastin may be involved in the formation of thin dumbbell-shaped tubules observed at the forming cell plate (34). These structures are apparently coated with a fuzzy layer that could be phragmoplastin polymers. Direct localization of phragmoplastin on such structure may be difficult due to the poor preservation of such structures (34). Similar structures have also been observed in tubular membrane invaginations in nerve terminals or isolated endosome vesicles formed in the presence of GTPγS (15, 16). That GTP hydrolysis may be delayed at vesicle-tubule-vesicle is suggested by the fact that a GTPase-minus mutant form of phragmoplastin remains in the Golgi bodies and is unable to reach to the cell plate during cytokinesis.[3] This property of phragmoplastin and the timing of GTP hydrolysis may be critical in forming tubular structures at the cell plate, which are necessary for making a fenestrated structure. The *KNOLLE* gene product that encodes a novel syntaxin (35) may be involved in the fusion of the vesicle-tubule-vesicle structures into stellated bodies, creating a fenestrated network that prevents vesicle-vesicle fusion.[4] Further characterization of phragmoplastin-associated proteins may reveal the mechanism by which such structures are formed during cell plate formation in plants. This unique process ensures the building of a flattened wall at cytokinesis.

[3] Z. Hong and D. P. S. Verma, unpublished data.
[4] D. P. S. Verma, submitted for publication.

Acknowledgments—We thank the Ohio State University *Arabidopsis* Biological Resource Center for providing us with yeast strains and cDNA library CD4-10. We thank Dr. A. J. Delauney for comments on the manuscript.

REFERENCES

1. Gu, X., and Verma, D. P. S. (1996) *EMBO J.* **15,** 695–704
2. Urrutia, R., Henley, J. R., Cook, T., and McNieven, M. A. (1997) *Proc. Natl. Acad. Sci. U. S. A.* **94,** 377–384
3. Kang, S. G., Jin, J. B., Piao, H. L., Pih, K. T., Jang, H. J., Lim, J. H., and Hwang, I. (1998) *Plant Mol. Biol.* **38,** 437–447
4. Smirnova, E., Shurland, D. L., Ryazantsev, S. N., and van der Bliek, A. M. (1998) *J. Cell Biol.* **143,** 351–358
5. Otsuga, D., Keegan, B. R., Brisch, E., Thatcher, J. W., Hermann, G. J., Bleazard, W., and Shaw, J. M. (1998) *J. Cell Biol.* **143,** 333–349
6. Gu, X., and Verma, D. P. S. (1997) *Plant Cell* **9,** 157–169
7. Dombrowski, J. E., and Raikhel, N. V. (1995) *Plant Mol. Biol.* **28,** 1121–1126
8. Park, J. M., Cho, J. H., Kang, S. G., Jang, H. J., Pih, K. T., Piao, H. L., Cho, M. J., and Hwang, I. (1998) *EMBO J.* **17,** 859–886
9. Shin, H.-W., Shinotsuka, C., Torii, S., Murakami, K., and Nakayama, K. (1997) *J. Biochem.* **122,** 525–530
10. Imoto, M., Tachibana, I., and Urrutia, R. (1998) *J. Cell Sci.* **111,** 1341–1349
11. Schmid, S. L., McNiven, M. A., and De Camilli, P. (1998) *Curr. Opin. Cell Biol.* **10,** 504–512
12. Klein, D. E., Lee, A., Frank, D. W., Marks, M. S., and Lemmon, M. A. (1998) *J. Biol. Chem.* **273,** 27725–27733
13. Nakayama, M., Yzaki, K., Kusano, A., Nagata, K., Hanai, N., and Ishihama, A. (1993) *J. Biol. Chem.* **268,** 15033–15038
14. Nakayama, M., Nagata, K., Kato, A., and Ishihama, A. (1991) *J. Biol. Chem.* **266,** 21404–21408
15. Hinshaw, J. E., and Schmid, S. L. (1995) *Nature* **374,** 190–192
16. Takei, K., McPherson, P. S., Schmid, S. L., and De Camilli, P. (1995) *Nature* **374,** 186–190
17. Sweitzer, S. M., and Hinshaw, J. E. (1998) *Cell* **93,** 1021–1029
18. McNiven, M. A. (1998) *Cell* **94,** 151–154
19. Carr, J. F., and Hinshaw, J. E. (1997) *J. Biol. Chem.* **272,** 28030–28035
20. Shin, H. W., Takatsu, H., Mukai, H., Munekata, E., Murakami, K., and Nakayama, K. (1999) *J. Biol. Chem.* **274,** 2780–2785
21. Smirnova, E., Shurland, D. L., Newman-Smith, E. D., Pishvaee, B., and van der Bliek, A. M. (1999) *J. Biol. Chem.* **274,** 14942–14947
22. Okamoto, P. M., Tripet, B., Litowski, J., Hodges, R. S., and Vallee, R. B. (1999) *J. Biol. Chem.* **274,** 10277–10286
23. Nevels, M., Wolf, H., and Dobner, T. (1999) *BioTechniques* **26,** 57–58
24. Jain, V. K., and Magrath, I. T. (1991) *Anal. Biochem.* **199,** 119–124
25. Kim, J., Harter, K., and Theologis, A. (1997) *Proc. Natl. Acad. Sci. U. S. A.* **94,** 11786–11791
26. Guan, K. L., and Dixon, J. E. (1991) *Anal. Biochem.* **192,** 262–267
27. Frangioni, J. V., and Neel, B. G. (1993) *Anal. Biochem.* **210,** 179–187
28. Melen, K., Ronni, T., Broni, B., Krug, R. M., von Bonsdorff, C. H., and Julkunen, I. (1992) *J. Biol. Chem.* **267,** 25898–25907
29. Shpetner, H. S., and Vallee, R. B. (1989) *Cell* **59,** 421–432
30. Maeda, K., Nakata, T., Noda, Y., Sato-Yoshitake, R., and Hirokawa, N. (1992) *Mol. Biol. Cell* **3,** 1181–1194
31. Takei, K., Mundigl, O., Daniell, L., and De Camilli, P. (1996) *J. Cell Biol.* **133,** 1237–1250
32. Schumacher, B., and Staeheli, P. (1998) *J. Biol. Chem.* **273,** 28365–28370
33. Takei, K., Haucke, V., Slepnev, V., Farsad, K., Salazar, M., Chen, H., and De Camilli, P. (1998) *Cell* **94,** 131–141
34. Samuels, A. L., Giddings, T. H., and Staehelin, L. A. (1995) *J. Cell Biol.* **130,** 1345–1357
35. Lauber, M. H., Waizenegger, I., Steinmann, T., Schwarz, H., Mayer, U., Hwang, I., Lukowitz, W., and Jurgens, G. (1997) *J. Cell Biol.* **139,** 1485–1493

Phragmoplastin Polymerizes into Spiral Coiled Structures via Intermolecular Interaction of Two Self-assembly Domains

Zhongming Zhang, Zonglie Hong and Desh Pal S. Verma

J. Biol. Chem. 2000, 275:8779-8784.
doi: 10.1074/jbc.275.12.8779